Physics of the Earth and Planetary Interiors 175 (2009) 63–77

Contents lists available at ScienceDirect

Physics of the Earth and Planetary Interiors

journal homepage: www.elsevier.com/locate/pepi

Amplification phenomena observed in downhole array records generated on a subductive environment

Ramon Verdugo*

Department of Civil Engineering, University of Chile, Blanco Encalada 2002, Santiago, Chile

ARTICLE INFO

Article history:
Received 3 April 2007
Accepted 3 March 2008

Keywords:
Site effect
Downhole array
H/V spectral ratio
Transfer function

ABSTRACT

The damage caused by earthquakes is strongly dependent on the local site conditions and, as a result, site characterization and amplification phenomenon have become a subject of considerable interest to engineers and seismologists. A vertical array in a soil deposit in Llolleo City, near the coast of Chile, has been installed, being somewhat unique in that it is located in a subduction zone environment. Because the coast of Chile is one of the most seismically active areas of the world, this array is expected to be particularly valuable because it may produce recordings of very strong and very long duration motions. The characteristics of this borehole array are presented first, which include pore water pressure measurements in clayey soils. Also some interesting aspects of the earthquakes recorded to date are described, which open a question about the suitability of one-dimensional analysis. In addition, the H/V spectral ratio proposed by Nakamura to estimate natural periods is analyzed. Microtremor measurements at the surface and the seismic events recorded by the seismic borehole array of Llolleo are used, looking both at the H/V spectral ratio of the motion recorded on the free surface and at the ratio of the response spectra of the motions at the surface and at bedrock. On the other hand, it is observed that the recorded dynamic pore pressures are controlled by the vertical accelerations, or compressional waves.

1. Introduction

Empirical evidence from earthquakes experienced all around the world has been conclusive in indicating that local geological and geotechnical conditions can play an important role on the characteristics of the shaking at the ground surface. Seismic amplifications and damage patterns observed during strong earthquakes present a great variability from one place to another, even over short distances, and some of these differences can be explained at times by the particular local ground conditions (Seed and Idriss, 1969; Aki, 1993; Borcherdt, 1994; Midorikawa et al., 1994, among others). Therefore, structures located on soil deposits of different geotechnical properties, in the same seismic area, can be subjected to seismic disturbances that may be quite different. For example, large amplitudes and long durations of ground motion have been observed on thick saturated unconsolidated materials, as found along the margins of San Francisco Bay during the 1906 earthquake (Borcherdt, 1970). An outstanding example of site effects is provided by the valley of Mexico City, where the ground motion has been amplified by a factor of 20 or more in many areas (Celebi et al., 1987; Singh and Ordaz, 1993). On the other hand, sites consisting of cemented soils, rock outcrops, or stiff soils in general, have consistently shown low seismic amplitudes and in some cases attenuation (Mohraz, 1976; Seed and Idriss, 1969; Seed et al., 1976, 1988).

Confirming what has been observed in other strong motions, it is possible to observe in the distribution of intensities and damage caused by the 1985 Chilean earthquake of magnitude 7.8, the existence of certain zones where the shaking effects were locally higher, regardless of epicentral distance, as shown Fig. 1 (Astroza et al., 1993). For example, intensities ranging from 7 to 10.5 were observed at sites in close proximity just north of the port of San Antonio. The analysis of the soil conditions consistently indicated that the higher intensities were reported at sites underlain by saturated soil deposits of sandy silt, silty sand and soft clay.

According to all the experience gained through field observations and by the accumulation of valuable data provided by modern seismic stations, site effects are completely accepted and, therefore, explicitly incorporated into seismic codes to better account for amplification phenomena (Borcherdt, 1994, 2002; Dobry et al., 1999; Dobry and Iai, 2000).

Nevertheless, in spite of the recent advances generated by earthquake geotechnical engineering there are still uncertainties to be investigated and resolved regarding the seismic amplification problem. Consequently, the first Chilean seismic station with a vertical array of borehole accelerometers and piezometers has been installed to permit measurements of the seismic amplitudes from

* Fax: +56 2 6892833.
E-mail address: rverdugo@ing.uchile.cl.

0031-9201/$ – see front matter © 2009 Elsevier B.V. All rights reserved.
doi:10.1016/j.pepi.2008.03.014

bedrock to the ground surface and their interrelation with pore water pressure variations. The location selected for the vertical array corresponds to an area that showed strong seismic amplification and heavy damage to houses during the 1985 Chilean earthquake, of magnitude 7.8.

During the operation of this array, 16 earthquakes of small to medium magnitude have been recorded, providing new insight about the amplification phenomenon. The analysis and interpretation of these data are presented.

Because the potential damage of earthquakes is strongly dependent on local site conditions, an adequate site characterization is a topic of considerable importance in seismic design. While there are a variety of geophysical methods to determine soil properties in situ, they all require special equipment to induce the disturbance, record the motions and process the data. The spectral ratio between the horizontal and vertical (H/V) spectra suggested by Nakamura (1989) provides an attractive procedure due to its simplicity and the rather short time needed for measurements (Nakamura, 1989; Field et al., 1990; Field and Jacob, 1995; Lermo and Chávez-García, 1993; Lachet and Bard, 1994; Saita et al., 2001). The H/V ratio can be used with seismic records obtained at one station located on the surface of the site under study or, as proposed by Nakamura, from microtremor measurements. Although this procedure seems promising, there is not a complete consensus yet about the reliability of the H/V spectral ratio on the estimation of the actual site response and several papers have indicated that more research is still needed (Bard, 1999; Bonilla et al., 1997; Konno and Ohmachi, 1998; Rovelli et al., 1991; Safak, 1991).

In order to gain additional insight about the applicability of the H/V spectral ratio to assess the seismic amplification of a site, microtremors (ambient vibrations) and seismic events recorded at the Llolleo borehole array are analyzed in this paper.

2. The Llolleo borehole array

This seismic array is located in a rather flat area close to the Pacific coast, west of Llolleo City, approximately 91 km west of Santiago as shown in Fig. 1. The seismic array consists of three force balance triaxial accelerometers SSA-320SS, two fast-response piezometers, and one GPS time receiver. The accelerometers were installed at the ground surface, at 24 m depth, and at 62 m depth, respectively. The accelerometer installed at 62 m depth was placed on the bedrock, penetrating 0.5 m into sound granite. The horizontal components of the accelerometers were aligned with an electronic compass in the north–south and east–west directions. The piezometers were installed at depths of 9.6 and 17.4 m on

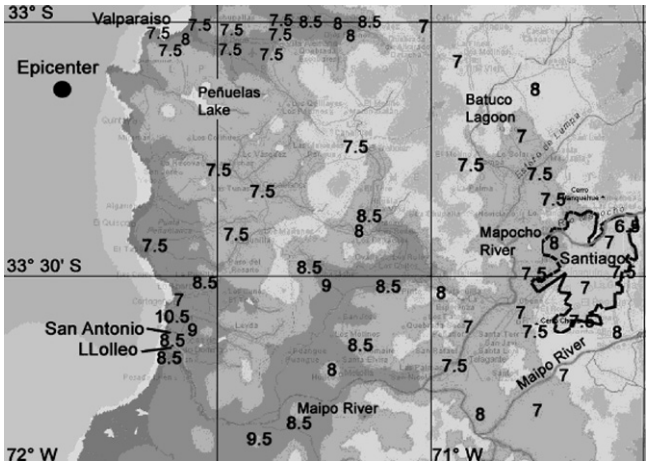

Fig. 1. Distribution of intensities. Chilean earthquake, 1985.

fine-grained soil layers. In this aspect the Llolleo borehole array is somewhat singular in having pore pressure measurements in clayey soils. Each instrument was installed at the bottom of a different borehole especially drilled for each instrument. The boreholes were separated from each other at a horizontal distance of about 3 m.

The data acquisition system continuously reads and stores the data coming from the 11 output channels associated with the three triaxial accelerometers and the two piezometers at a sampling rate of 50 readings per second, leading to a Nyquist frequency of 25 Hz, which is considered acceptable for the analysis and in the other hand, it reduced the cost of the equipment. The hard disk of the computer is partitioned in two areas, so all the readings are continuously stored in one part of the hard disk in a ring buffer. When the total capacity of this part of the hard disk is exceeded, the new data are overwritten in the ring buffer from the beginning, so a continuous process of data acquisition is maintained. The level of the horizontal accelerations registered by the accelerometer located on the ground surface is continuously checked throughout a time window and compared with a triggering acceleration of 0.001 g. When this level of acceleration is exceeded, a file with a name corresponding to the date and time of the event is created. In this file all the readings are stored, considering a period of time starting 30 s before the triggering acceleration was exceeded and finishing 15 min after. This period of 15 min allows measurements of the main part of the dissipation of pore water pressure, which is also an important parameter to be studied.

3. General geological conditions at the site

From a geological point of view, Chile is characterized to the south of parallel 33°, by the existence of three morphostructural units running parallel to each other with a north–south orientation. From east to west, these units are the Andes Mountain Range, the Central Valley and the Coastal Mountain Range. The city of Llolleo is located in the western part of the Coastal Mountain Range, where tertiary intrusive rocks, quaternary in-shore soil deposits and alluvial soil deposits associated with the El Sauce Creek and Maipo River can be observed.

The main geological structures in the area are related to old faults that have affected tertiary intrusive rocks. The most important fault is oriented north–northwest and it seems to control the direction of some parts of the Maipo River. Another fault, oriented northwest, is located to the south of Llolleo City, and governs the direction of the Maipo River where it reaches the Pacific Ocean.

The seismic array is located west of Llolleo City. There, quaternary alluvial soil deposits consist of sands, gravels, clays and silts, with a planar and horizontal stratification. In this area, below a depth of 45 m, calcareous sediments consisting of shells can be found in soil layers of sandy and gravelly materials. The observed sequence of soils and shells can be interpreted as an in-shore soil deposit, mainly controlled by sea action. Above this level, the soil strata are finer and consist mainly of silty and clayey materials, reflecting a change in the energy of deposition, which is likely associated with past sea level variations. The upper part of the soil deposit consists of sandy and silty materials. A general view of the sediments that can be observed at the surface is provided in Fig. 2.

4. Geotechnical properties of the site

Soil conditions at the site were investigated using the boreholes drilled to install the sensors and by means of an additional borehole specifically carried out for this purpose. Standard Penetration Tests (SPT) were performed to assess geotechnical properties and "undisturbed" samples were retrieved by means of Shelby tubes for

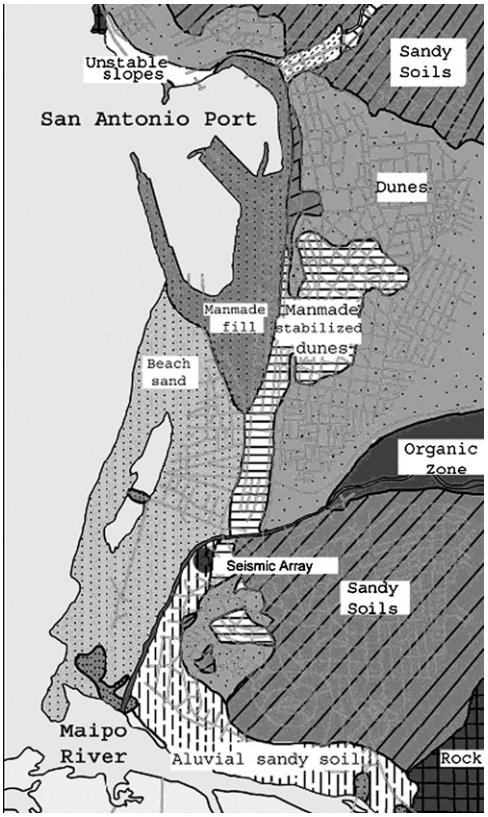

Fig. 2. Local geology.

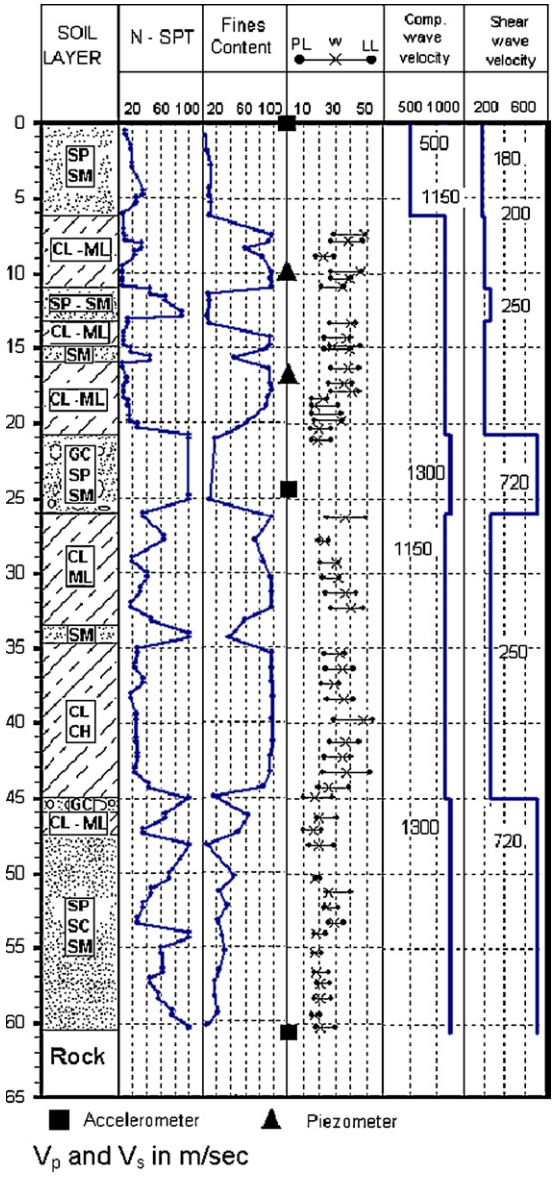

Fig. 3. Geotechnical properties of the site.

laboratory testing. To evaluate the profile of shear wave velocities at low level of strain, Down-Hole tests were carried out every 5 m down to bedrock. Additionally, Cross-Hole tests were performed up to a depth of 20 m, resulting very similar values of the shear wave velocities.

The geotechnical characterization of the site is summarized in Fig. 3, where penetration index (N-SPT), fines content (percentage of soil particles smaller than 0.075 mm), Liquid Limit (LL), Plastic Limit (PL), natural water content (ω), compressional wave velocity, (V_p) and shear wave velocity (V_s) are presented. The Atterberg Limits (LL and PL) indicate that most of the fines are constituted basically by low plastic silt (ML) and clay (CL). The natural water content is closer to the LL than the PL, suggesting that these fines are normally consolidated, in other words, they are in a soft condition, which is reflected by the low shear wave velocities. The N-SPT results show that sandy layers present higher penetration index, while silty and clayey layers present quite low penetration index, which is also reflected in the values of the shear wave velocities. The profile indicates the existence of bedrock at 60.5 m depth and strata composed by a layered structure of soils. It is possible to identify a shallow sandy soil deposit, 6.2 m thick, with a shear wave velocity around 180 m/s. From 6.2 to 11 m depth, a layer of low plastic clay and silty material is identified with a characteristic shear wave velocity of 200 m/s. Then a sandy soil layer with a shear wave velocity of 250 m/s is observed. Below this and down to 20.8 m, an alternate sequence of layers of clay, silt and sand can be detected, with an average shear wave velocity close to 200 m/s. Then, down to 26 m depth, a stiff layer of gravelly soil with a shear wave velocity of 714 m/s is observed. From 26 to 45 m, a sequence of clay, silty and sandy soil layers, appears again with a shear wave velocity of approximately 250 m/s. Finally, there is a stiff silty sand deposit, characterized by a shear wave velocity of 720 m/s. Beneath this bottom layer, the granite bedrock can be found. It is important to bear in mind that the accelerometer located in the bedrock was installed at a depth of 62 m in competent granite. The shear wave velocity of this rock is estimated around 1800 m/s. The water table was found at a depth of 6 m.

5. Seismic characteristic of the area

The central part of Chile, where the borehole array is located, is regularly subjected to different type of seismic events. From an engineering point of view, the most important earthquakes in this area are related to the subduction of the oceanic Nazca plate below the South American continental plate. An average displacement of 9 cm per year of the Nazca plate relative to and against the continental plate is normally estimated. In this subductive seismic environment, the central part of Chile located between latitudes 32.5° S and 34° S has been exposed to a notable periodicity of large earthquakes. The years of occurrence of these major events have been reported as follows: 1575, 1647, 1730, 1822, 1906 and 1985. This sequence results in an average recurrence interval of 82 ± 6 years.

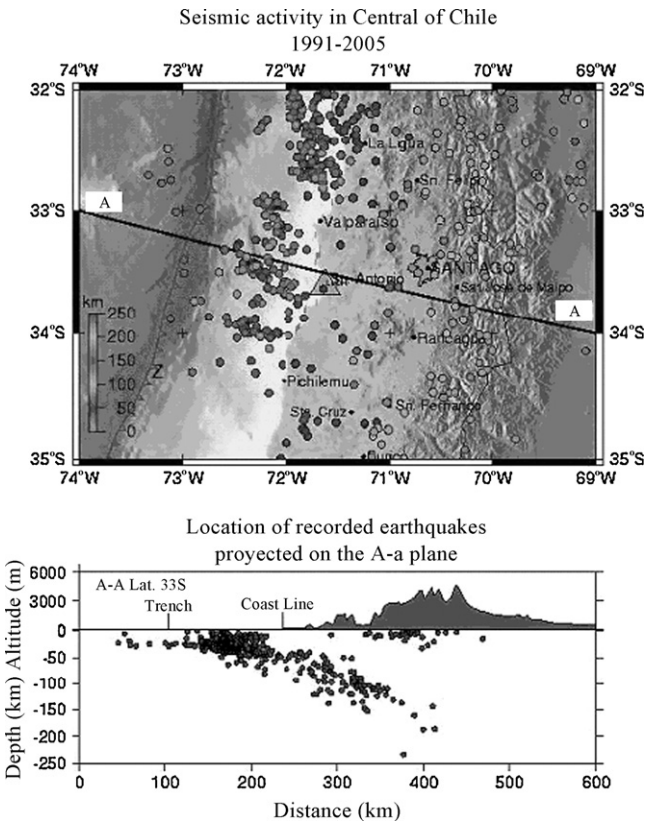

Fig. 4. Seismic activity in central part of Chile.

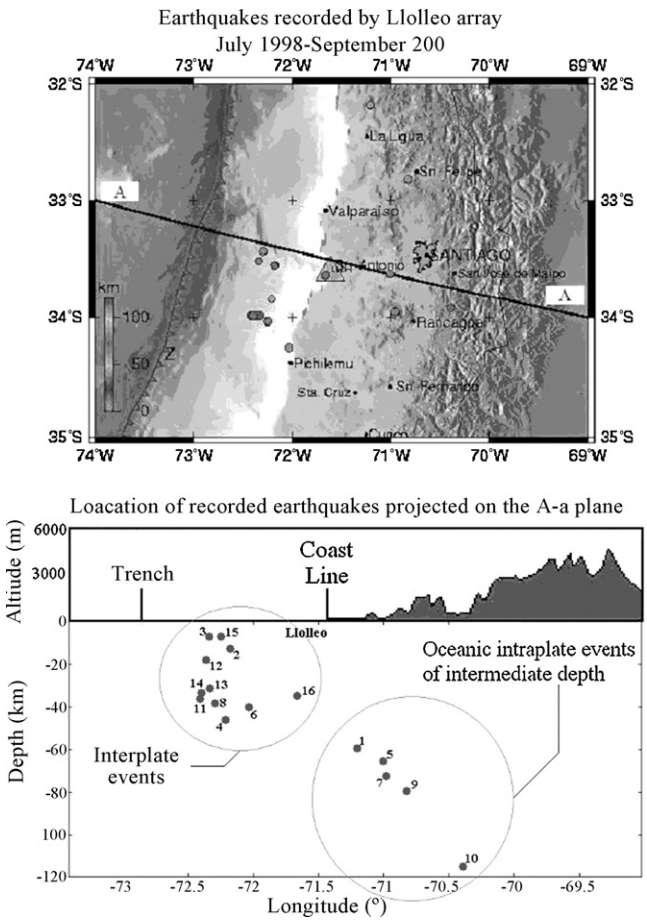

Fig. 5. Location of recorded earthquakes.

The seismic activity between latitudes 32.5° S and 35° S associated with events larger than magnitude 4 and recorded since 1991 by the Chilean Seismological Service of University of Chile is shown in Fig. 4. To visualize the distribution of the hypocenters according to their depth, all the seismic events located in this area have been projected to the vertical plane passing through the A–A axis. Most of the seismicity occurs between the oceanic trench and the coast, following Benioffís plane. Nevertheless, it is important to point out that a rather shallow seismicity into the continental plate and below Los Andes Range is observed. It is also worth mentioning that seismic activity is frequent beyond the oceanic trench.

Therefore, the Llolleo seismic borehole array is located in an active seismic region where different types of earthquakes could be eventually recorded. These types of earthquakes are associated with different seismic sources and also different rupture mechanisms.

6. Earthquakes recorded to date

During the operation of the Llolleo seismic array 16 seismic events have been recorded, the main features of which are indicated in Table 1. The magnitudes of these events are between 4.2 and 6, with distances from the station to the epicenters in the range of 4–164 km. The maximum horizontal acceleration that has been recorded at the ground surface of the station is 0.14 g, while the maximum horizontal acceleration recorded at the bedrock is 0.017 g.

The location of the hypocenters of the recorded earthquakes is presented in Fig. 5. It is interesting to observe that the recorded seismic events can be grouped into those that originated in the plate contact and those likely created inside the oceanic plate that is subducting the continental plate.

The acceleration time histories of typical small seismic events recorded to date are shown in Fig. 6. A first arrival of P-waves is observed that is followed by a main package of S-waves, and afterwards a typical coda is manifested. It is observed that as the motion propagates upwards, the amplification of the shaking is readily apparent, phenomenon that has been systematically seen in all the recorded seismic events.

7. Recorded dynamic pore water pressure

An important aspect of seismic soil amplification is related to the increments of pore water pressure due to cyclic shear stress reversal caused by the seismic disturbance. The buildup of pore water pressure reduces the effective stresses and consequently the soil stiffness, and can cause a sudden drop in the strength, or a significant degradation of stiffness in the case of loose cohesionless material. This extreme situation is associated with the occurrence of the liquefaction phenomena, manifested as flow failure or cyclic mobility (Casagrande, 1975; Seed, 1987; Ishihara, 1993).

In the area of the Llolleo array, the past experience left by strong earthquakes has shown evidence of liquefaction in some sandy soil deposits along the Maipo riverside. However, in the vicinity of the borehole station only heavy damage in housing have been observed, without sign of liquefaction. Nevertheless, high pore pressures would be expected in the rather loose sandy soil materials identified in the top 6 m in the type of strong shaking anticipated in the future in this highly active area. It is also considered of great importance to obtain new insight into the dynamic pore water changes that may occur in soft saturated fine materials. Consequently, two piezometers were installed in the soil deposits at depths of 9.6 and 17.4 m, embedded in soft soils characterized by N-SPT values less than 10

Table 1
Recorded earthquakes.

Date (d-m-y)	Local time	Magnitude	Depth (km)	Epicentral distance (km)	Latitude,longitude	Location	Maximum accelerations (m/s^2)		
							Vertical	N–S	E–W
03-08-1999	16:24	4.8	79.5	115	32°49,02′	S	0.0544	0.1224	0.0845
					70°49,32′	M	0.0214	0.0214	0.0259
						B	0.0083	0.0102	0.0096
04-04-1999	21:04	4.5	65.5	59	33°37,5′	S	0.1467	0.3331	0.2489
					71°0,12′	M	0.0528	0.1067	0.0830
						B	0.0188	0.0206	0.0458
06-04-1999	7:45	4.9	40.2	82	34°15,24′	S	0.2626	0.5368	0.4677
					72°2,22′	M	0.1273	0.1581	0.1909
						B	0.0338	0.0732	0.0592
10-07-1998	13:58	4.8	59.4	164	32°10,86′	S	0.0459	0.0930	0.0893
					71°12,3′	M	0.0188	0.0243	0.0310
						B	0.0065	0.0082	0.0072
10-10-1998	1:16	4.8	12.9	65	33°33,06′	S	0.0405	0.1166	0.0829
					72°10,86′	M	0.0190	0.0287	0.0304
						B	0.0125	0.0092	0.0131
16-06-2000	7:55	6.0	115.2	133	33°55,08′	S	0.5171	1.3750	0.9436
					70°23,46′	M	0.2086	0.4329	0.3104
						B	0.0734	0.0902	0.1689
16-10-1998	20:03	4.4	7.2	64	33°30,84′	S	0.0062	0.0112	0.0124
					72°20,46′	M	0.0031	0.0045	0.0036
						B	0.0020	0.0016	0.0010
17-01-1999	15:18	4.4	46	65	33°50,22′	S	0.0689	0.1156	0.0804
					72°12,72′	M	0.0196	0.0288	0.0252
						B	0.0070	0.0106	0.0150
25-06-1999a	11:08	4.4	72	67	33°55,2′	S	0.0320	0.0807	0.0765
					70°58,68′	M	0.0124	0.0188	0.0215
						B	0.0042	0.0083	0.0099
25-06-1999b	17:15	4.7	38.5	67	33°25,8′	S	0.0277	0.0484	0.0705
					72°17,88′	M	0.0127	0.0161	0.0303
						B	0.0047	0.0058	0.0046
07-09-2004a	10:57	5.3	36.3	85	33°58′8″	S	0.0603	0.1068	0.1911
					72°25′4″	M	0.0272	0.0501	0.0615
						B	0.0106	0.0168	0.0128
07-09-2004b	12:33	5.3	17.9	80	33°59′41″	S	0.0969	0.1033	0.1559
					72°21′7″	M	0.0258	0.0450	0.0360
						B	0.0116	0.0113	0.0126
08-09-2004a	8:16	5.1	31.6	77	33°59′27″	S	0.0503	0.0730	0.0833
					72°19′19″	M	0.0150	0.0259	0.0220
						B	0.0073	0.0085	0.0070
08-09-2004b	8:06	4.7	33.5	83	33°59′56′	S	0.0320	0.0661	0.0827
					72°23′56″	M	0.0120	0.0169	0.0191
						B	0.0069	0.0056	0.0062
09-09-2004	8:47	4.8	7.1	76	34°1′19″	S	0.0420	0.0731	0.0617
					72°15′10″	M	0.0132	0.0182	0.0189
						B	0.0066	0.0059	0.0055
10-09-2004	9:00	4.2	35	4	33°37′51″	S	0.1147	0.1255	0.1793
					71°39′10″	M	0.0164	0.0240	0.0285
						B	0.0117	0.0145	0.0240

blows per foot, a fines content greater than 95% and classified as clay and silt of low plasticity (CL-ML).

Typical acceleration time histories of all components are presented in Fig. 7. For this earthquake the dynamic pore water pressures measured during the seismic event are shown in Fig. 8. Interestingly, it is observed that the dynamic pore pressure follows the shape of the vertical acceleration time history recorded at 24 m depth. To study the correspondence between the dynamic pore pressures and the vertical accelerations, a cross-correlation analysis was performed using the whole signal. The results are presented in Fig. 9 and they reflect the apparent correlation among these signals. Thus, it is possible to conclude that the recorded dynamic pore water pressures in fine-grained soils are associated with compressional waves traveling through the saturated soil deposit. It is very important to point out that the recorded earthquakes are rather small and probably because of this no pore pressure build-up has been observed yet. The highest correlation between the bedrock vertical acceleration and the pore water pressure recorded at 9.6 m depth, is observed at $\tau = 0.22$ s. This value should be associated with the time needed by the compressional wave to travel from the accelerometer to the piezometer, however, from these results it is possible to indicate that initially the dynamic pore water pressure is affected by the complete signal and thereafter, it is mainly controlled by the vertical accelerations. Additionally, it is observed a correlation period of about 0.23 s, which matches the predominant period observed in the vertical acceleration recorded at 24 m depth.

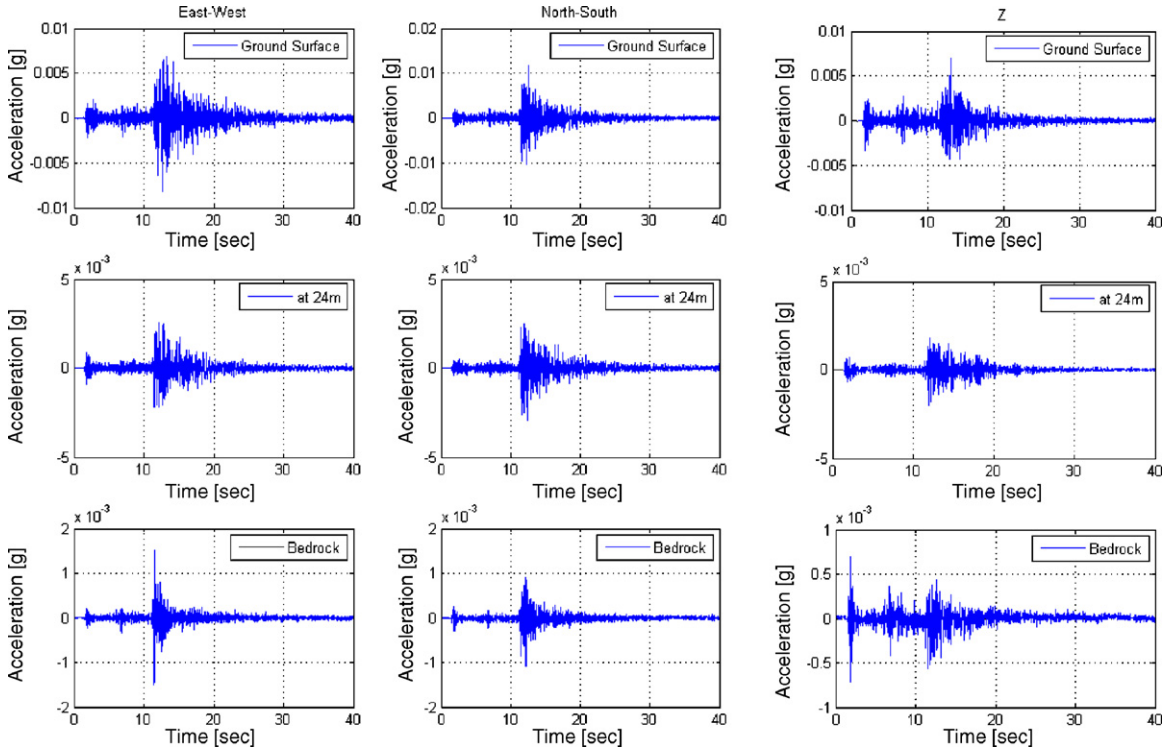

Fig. 6. Typical acceleration time history of a small recorded seismic event.

8. Amplification in terms of peak accelerations

All the recorded seismic events clearly show a significant amplification of the acceleration amplitudes from bedrock to the ground surface. For the recorded earthquakes with horizontal peak acceleration at the ground surface greater than 0.005 g, the peak accelerations normalized by the peak accelerations at the bedrock are presented in Figs. 10–12. It can be seen that the relatively weak recorded motions are significantly amplified from the bedrock to the ground surface, being especially augmented near the surface. For the geotechnical conditions of the Llolleo site, and for the level of shaking that has been recorded, the amplification factor for peak horizontal acceleration is in the range of 1–7, for the sector going from the bedrock to a depth of 24 m. This factor increases to the range of 4–16, for the total domain comprised between the bedrock and the ground surface. These results suggest that most of the phenomenon of amplification is developed near the ground surface, probably in the upper 20 m. The amplification phenomenon is ana-

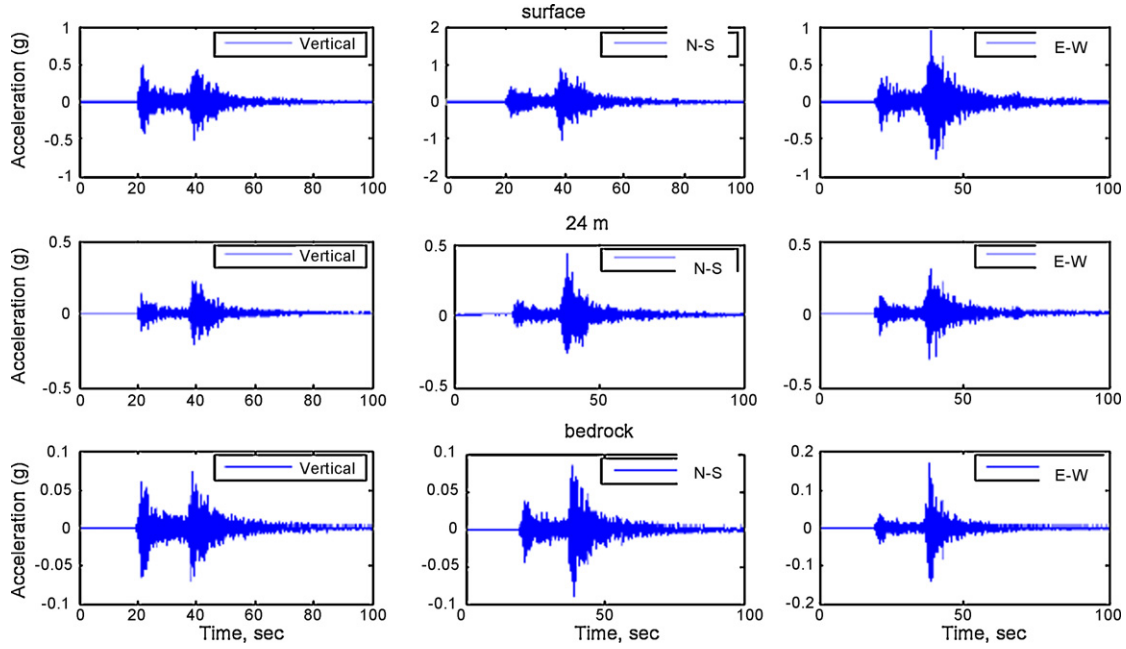

Fig. 7. Acceleration time history of a recorded seismic event 16.06.00.

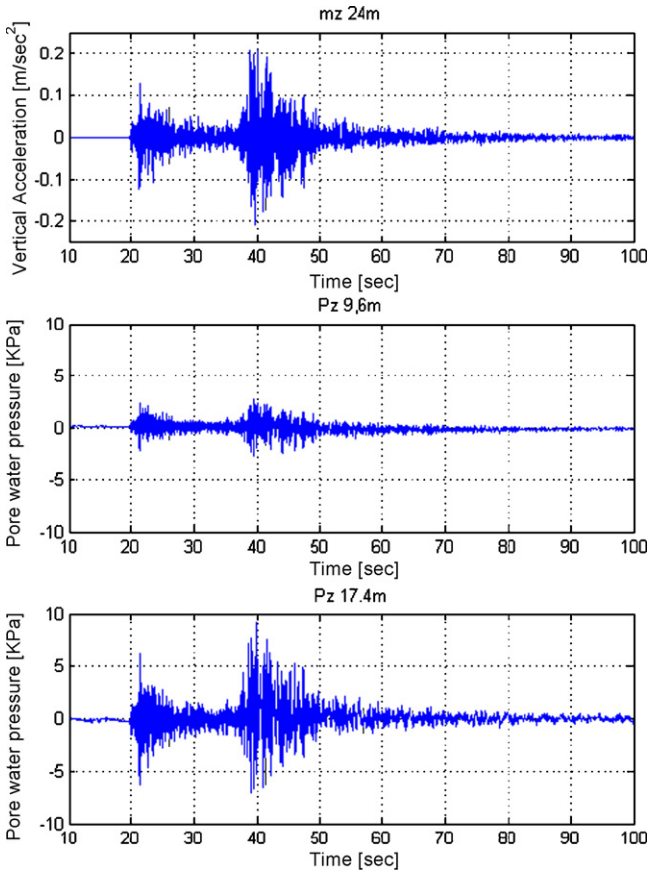

Fig. 8. Typical pore water pressure response recorded at 9.6 and 17.4 m depth and vertical acceleration recorded at 24 m depth. Seismic event 16.06.00.

lyzed in a more comprehensive manner throughout the analysis of empirical transfer functions computed in the frequency domain using the recorded motions and ambient noise as shown below.

Regarding the amplification of vertical acceleration, the measurements indicate a factor in the range of 2–4, for the deepest sector located between the bedrock and a depth of 24 m. For the total soil deposit, the amplification factor is in the range of 4–10. Again, the main part of the amplification takes place in the top 20 m, but it is less pronounced than that observed for horizontal accelerations.

9. Empirical transfer functions from base to ground surface

Among the different approaches to model the cyclic soil response, the most popular is based on the assumption of linear hysteretic soil behavior. This type of modeling has been extensively used in conjunction with the theory of unidimensional shear wave propagation, adjusting soil properties on the basis of the computed strains to simulate nonlinear soil behavior. This approach has provided most of the concepts used in the framework of soil amplification.

At the surface of the soil deposit takes place the so-called free surface motion, and its prediction in terms of amplitude, duration and frequency contents, is the goal of earthquake geotechnical engineering. Considering a halfspace with a one-dimensional train of shear waves propagating vertically throughout a homogenous soil deposit and assuming hysteretic soil behavior, the amplification of the amplitude of a sinusoidal motion (acceleration, velocity and displacement) from a rigid bedrock to the free surface at any frequency, Ω, is given by (Roësset and Whitman, 1969):

$$A(\Omega) = \frac{1}{\sqrt{\cosh^2\alpha\,\cos^2\beta + \sinh^2\alpha\,\sin^2\beta}} \tag{1}$$

where:

$$\alpha = \frac{H\Omega}{\sqrt{G/\rho}}\sqrt{\frac{\sqrt{1+4D^2}-1}{2(1+4D^2)}} \tag{2}$$

and,

$$\beta = \frac{H\Omega}{\sqrt{G/\rho}}\sqrt{\frac{\sqrt{1+4D^2}+1}{2(1+4D^2)}} \tag{3}$$

Here, H and G and ρ represent the thickness of the soil deposit, the shear modulus of the soil and the mass density of the soil, respectively. D corresponds to the damping ratio defined as the area of the hysteretic loop associated with a complete cycle of loading–unloading–reloading divided by the theoretical elastic energy applied to the loading cycle times 4π (Seed and Idriss, 1970; Ishihara, 1982). Furthermore, for the undamped condition the fundamental period is given by:

$$T = \frac{4H}{V_s} \tag{4}$$

where V_s represents the shear wave velocity and its relation with the shear modulus is given by $G = \rho(V_s)^2$.

The function $A(\Omega)$ can be interpreted as the amplification function of a soil deposit subjected to a sinusoidal acceleration at bedrock (bottom) with a frequency Ω. It would be also theoretically the ratio of the amplitudes of the Fourier Transforms of the motions recorded at the free surface and at the bedrock if these motions were caused by vertically propagating shear waves. The ratio of the two Fourier Transforms is the transfer function, a complex function of frequency. The amplification function is thus the amplitude of the transfer function.

For a soil deposit consisting of soil layers of different properties, the above expressions are valid for each layer and the boundary conditions at the interfaces have to be incorporated. The resultant explicit solution for the amplification function becomes too long, even for two layers, but the numerical computation remains straightforward and simple (Roësset and Whitman, 1969; Roësset, 1977). According to the 1D theory it is interesting to notice that for vertically propagating waves and linear soil behavior, the transfer function is only a function of the soil properties and the thickness of the soil layers, and therefore, it represents the site effect, regardless of the characteristics of the shaking. However, it is important to bear in mind that shear modulus and damping ratio are strain dependent, and therefore, controlled by the intensity of shaking, which means that the transfer function should be also dependent on the level of the seismic event.

The amplification function for vertical motion caused by vertically propagating P waves would be given by the same expression replacing the shear modulus G by the constrained modulus of the material.

Fig. 13 shows the theoretical amplification function for vertically propagating shear waves assuming linear elastic soil behavior for the soil properties shown in Fig. 3. It can be seen that the first natural period in shear has a value of $T_{s1} = 0.74$ s and the second a value of $T_{s2} = 0.27$ s.

On the other hand, with available data at the surface as well as at bedrock, it is possible to obtain experimental amplification functions simply dividing the amplitudes of the Fourier transforms of the motions recorded at the free surface and at bedrock. However, in the present analysis, the ratio of the undamped velocity response

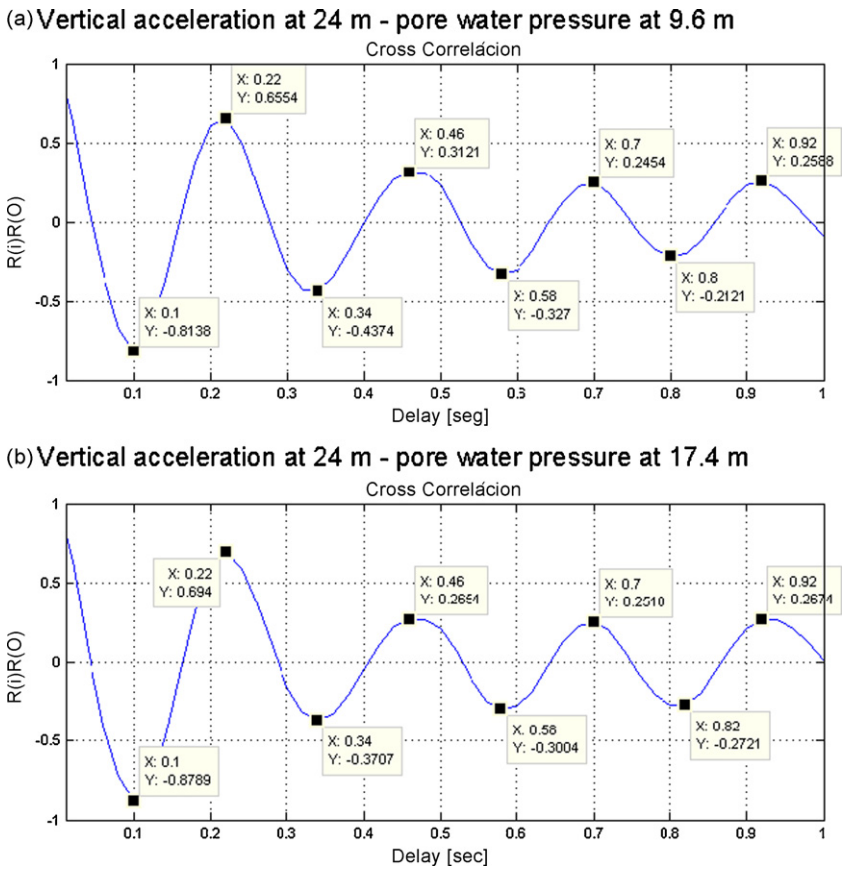

Fig. 9. Cross-correlation analysis between the pore water pressures recorded at 9.6 and 17.4 m and the vertical acceleration recorded at 24 m depth. (a) Vertical acceleration at 24 m—pore water pressure at 9.6 m. (b) Vertical acceleration at 24 m—pore water pressure at 17.4 m.

spectra of the two records has been used. As shown by Hudson (1956, 1979), the undamped velocity response spectrum, given by:

$$\left|x(t)\right|_{\max} = \sqrt{\left[\int_0^{t^*} a(\tau)\cos\omega\tau\,\mathrm{d}\tau\right]^2 + \left[\int_0^{t^*} a(\tau)\sin\omega\tau\,\mathrm{d}\tau\right]^2} \quad (5)$$

is an upper bound of the Fourier amplitude spectrum:

$$\mathrm{FA}(\omega) = \sqrt{\left[\int_0^{L} a(t)\cos\omega t\,\mathrm{d}t\right]^2 + \left[\int_0^{L} a(t)\sin\omega t\,\mathrm{d}t\right]^2} \quad (6)$$

and the values of the peaks are almost identical in most cases. A comparison between the amplification function and the ratio of response spectra has been provided by Sarrazin et al. (1969).

The ratio of response spectra are used here because it has a stronger engineering meaning in relation to damage to structures, because the resulting data are less sensitive to noise and because the peaks are easier to identify. Others researchers have also adopted the pseudo-velocity response spectra in their analysis of relative amplification factors across an array, as reported by Field and Hough (1997).

For each horizontal component, N–S and E–W, the response spectra at the ground surface and at the bedrock were computed

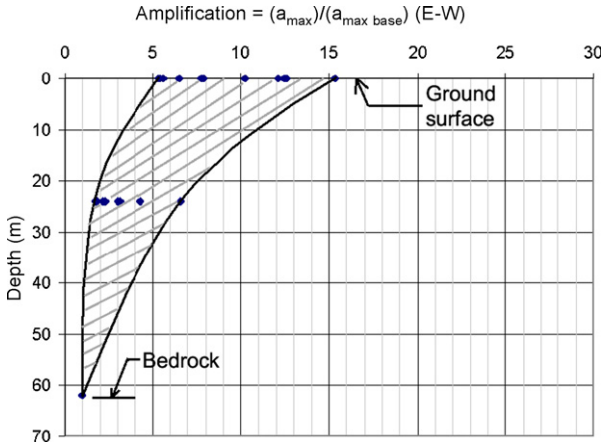

Fig. 10. Amplification of peak horizontal acceleration (E–W).

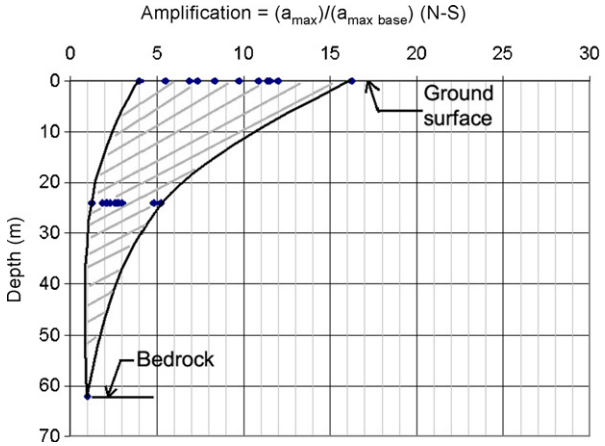

Fig. 11. Amplification of peak horizontal acceleration (N–S).

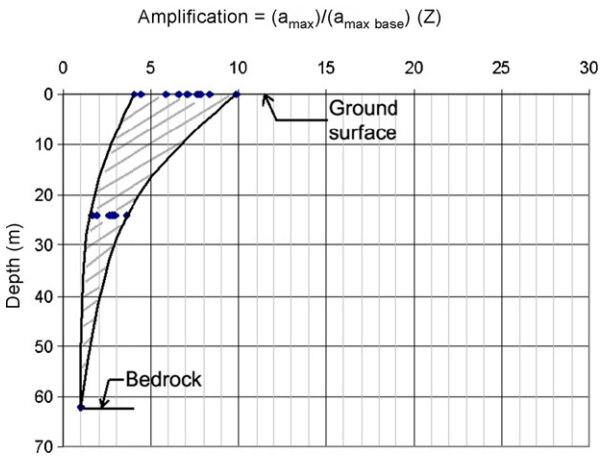

Fig. 12. Amplification of peak vertical acceleration.

and the corresponding ratios used to evaluate the empirical transfer functions for each recorded seismic event. Fig. 14a and b shows the results for the N–S and E–W components, respectively. As can be observed, different transfer functions have been obtained for each recorded earthquake, and also when the two horizontal components are analyzed for any particular earthquake, the resulting transfer functions are rather distinct, presenting peaks of amplification at different periods. In general, it is possible to identify amplification peaks at periods around 0.12, 0.23, 0.45, 0.52 s. These results suggest that depending on the frequency content and singularities of the input signal at the bedrock, different transfer functions can be obtained. The idea of showing the individual transfer functions is to be observed how different can be some of these functions, which is hidden by the use of averages. Nevertheless, in terms of an average it is possible to expect a more unique transfer function that represents the site effect. Accordingly, the average transfer function of the Llolleo site was computed. Trying to take into account the effect of noise and any potential bias introduced by the application of a particular calculation, the arithmetic average at each frequency and the geometric average at each frequency were computed. The mathematical expression used to evaluate the geometric average, TF_{GA} is given by:

$$\log_{10}(TF_{GA}) = \frac{1}{N}\sum_{i=1}^{N}\log_{10}(TF_i) \tag{7}$$

where TF_{GA} represents the geometric average of the transfer functions, N corresponds to the number of seismic events that in this case are 16, and TF_i represents the transfer function obtained for each recorded earthquake. The average empirical transfer functions obtained by these procedures were almost identical. The resulting average functions for each horizontal direction are shown in Figs. 15 and 16, and the resulting average of all the data in both directions is presented in Fig. 17. As can be observed, these results suggest that not only one fundamental frequency, or period, is associated with the main amplification of the input motion from the bedrock to the ground surface. To the contrary, these results indicate that the average transfer function reflects several frequencies, or periods, where the input motion is strongly amplified. According to the results presented in Fig. 17, the first three most relevant periods are: 0.45, 0.23 and 0.14 s. It is interesting to realize that the first period of 0.45 s is coincident with the natural period considering only the upper 20 m of soil layers.

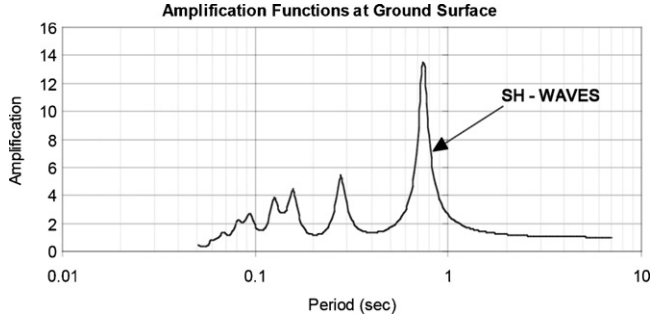

Fig. 13. Amplification function associated with SH waves.

According to these empirical results obtained from rather small ground motions, the site effect is manifested in a broad band of frequencies, all of which should be incorporated into the conceptualization of the actual amplification phenomenon. If the current one-dimensional analysis is considered, it is important to include the first 3–4 fundamental periods of vibration to cover the range of periods where the site effect would be predominant. Depending upon the genesis and path of each earthquake, any of these periods could become predominant. Therefore, more research is needed in order to find the particular features of an earthquake that amplify one or another frequency of a soil deposit.

10. The use of H/V spectral ratio

An alternative and attractive empirical procedure to estimate the transfer function of a site corresponds to the evaluation of the ratio between the amplitude spectrum of the horizontal component of motion and the amplitude spectrum of the vertical component of motion. This is so because it needs only one station, located at the site under study, so any potential distortion originated by an inappropriate reference station on rock outcrop is avoided. However, as is shown and discussed with the results of this research, the fundamental assumptions of the H/V procedure are not completely satisfied by the actual observed seismic response of soil deposits. The H/V spectral ratio with one station at the site was originally applied by Nakamura (1989) using microtremor records, and later several studies have shown the limitation and capability of this simple procedure (see for example the comprehensive studies reported by Bard, 1999; Lachet and Bard, 1994; Field et al., 1990; Field and Jacob, 1993, 1995; Lermo and Chávez-García, 1993). The H/V spectral ratio was defined by Nakamura as:

$$TF_{HW} = \frac{S_{HS}}{S_{VS}}\frac{S_{VB}}{S_{HB}} \tag{8}$$

where S_{HS}, S_{HB} represent the amplitude spectra of the horizontal motions at the surface and at the base of the soil stratum, respectively. While S_{VB} and S_{VS} represent the amplitude spectra of the vertical motions at the surface and at the base of the soil stratum, respectively. Based on data obtained by microtremor measurements at two different sites, the ratio, S_{HB}/S_{VB}, obtained by Nakamura suggested a value of around unity for a wide range of frequencies (this hypothesis is checked below with the available data recorded at the bedrock). Then, the transfer function can be evaluated as:

$$TF_{HW} = \frac{S_{HS}}{S_{VS}} \tag{9}$$

Replacing the microtremor measurements by seismic records, this procedure has been extended to evaluate site effects by means of only one seismic station at the ground surface. Using the intense shear wave part of the records, good results for the fundamentals frequencies computed by the H/V procedure have been reported (Lermo and Chávez-García, 1993; Bonilla et al., 1997).

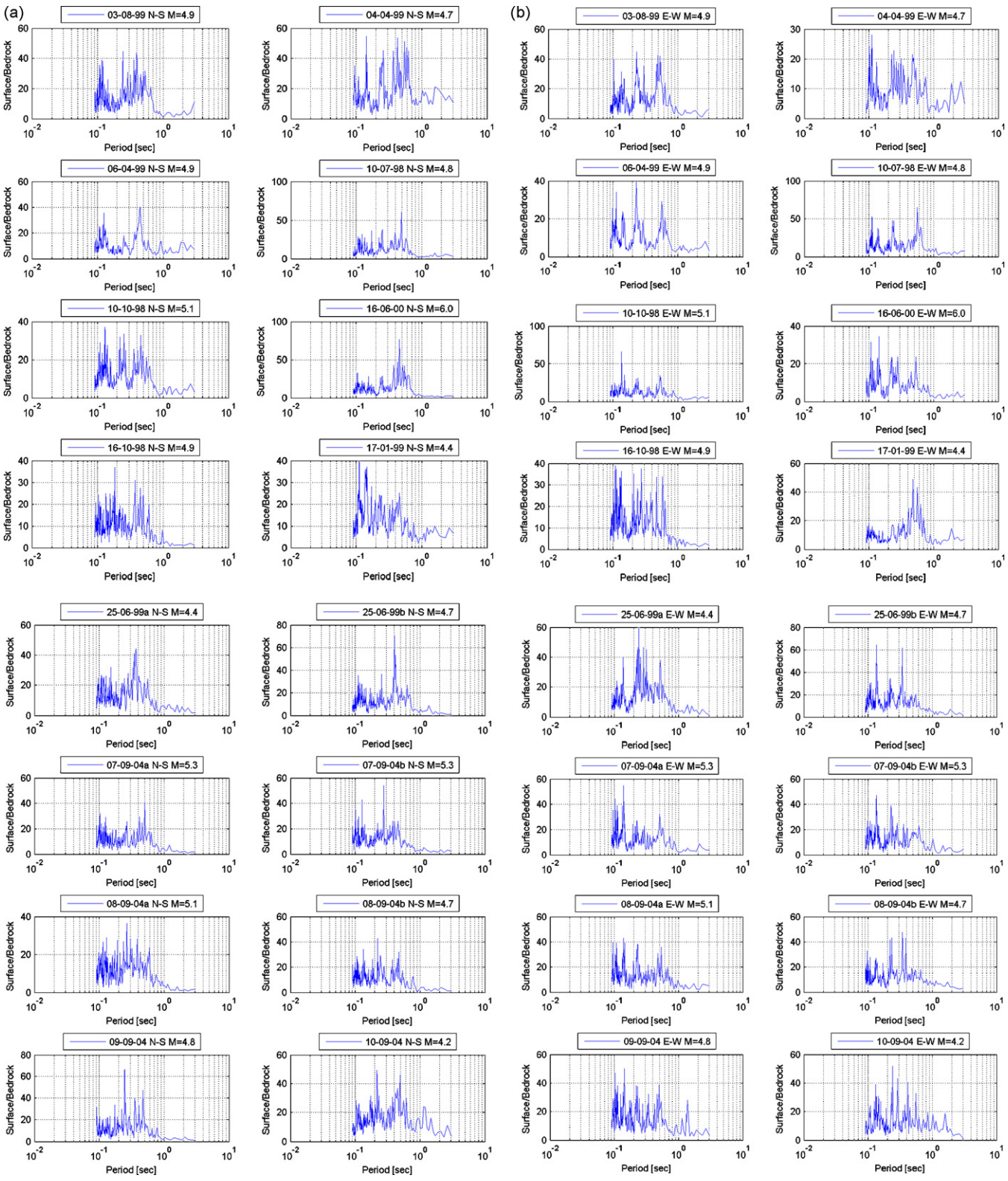

Fig. 14. (a) Empirical transfer function ground surface–bedrock (N–S). (b) Empirical transfer function ground surface–bedrock (E–W).

The seismic events recorded at the Llolleo array have been processed and the H/V spectral ratio has been computed. In addition, microtremor measurements were performed to compute the H/V spectral ratio. These results are compared with the transfer functions computed directly from the data of the borehole array.

11. H/V spectral ratio computed from microtremor measurements

Microtremor measurements were recorded at the site of the array. The instrumentation used for these purposes consisted of a triaxial array of seismometers with a flat response between 1 and

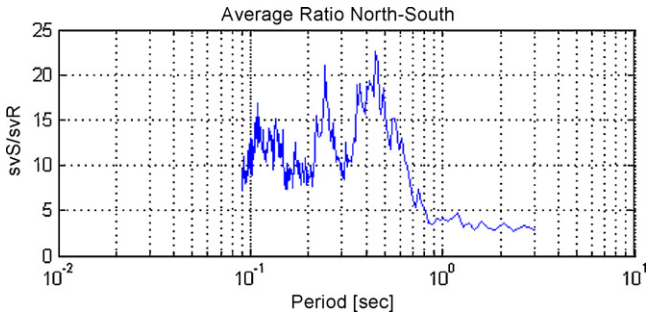

Fig. 15. Average empirical transfer function in the N–S direction.

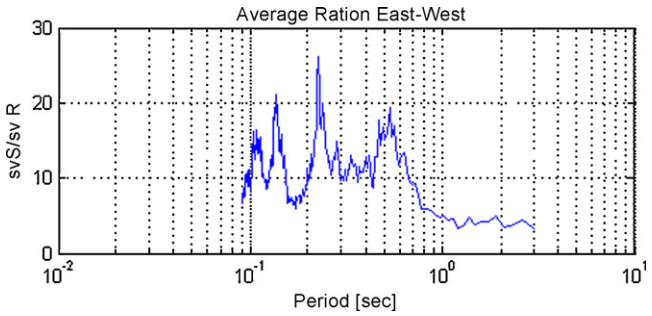

Fig. 16. Average empirical transfer function in the E–W direction.

300 Hz connected to a 16 bit digital analog converter. The sampling rate was set at 200 samples per second and a butterworth filter was used to eliminate aliasing. The total recording time was 3 h in three 1 h consecutive records. Typical records of ambient velocity are shown in Fig. 18.

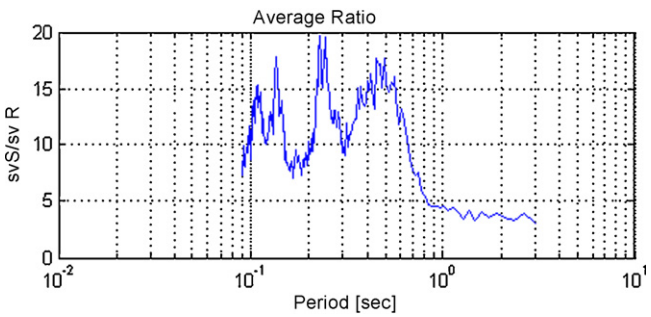

Fig. 17. Average empirical transfer function of the site.

The time records were inspected and segments with high transient disturbances were eliminated from the process. The Power Spectral Density (PSD) was obtained with the Welch method of averaging. Segment selection for processing was performed with a Welch window of 10 s duration. No overlapping of window segments was used.

During the measurements of the ambient vibrations, the horizontal sensors were oriented North–South (x) and East–West (y). In order to investigate any possible directional effect of the ambient vibrations in the horizontal plane, four different horizontal power spectral densities were calculated to evaluate the H/V ratios. First, the power spectral densities were computed independently for the horizontal vibrations recorded in the North–South direction (H_x) and East–West direction (H_y). A third power spectral density was evaluated as a combination of these two as:

$$\mathrm{RM} = \sqrt{\frac{H_x^2 + H_y^2}{2}} \tag{10}$$

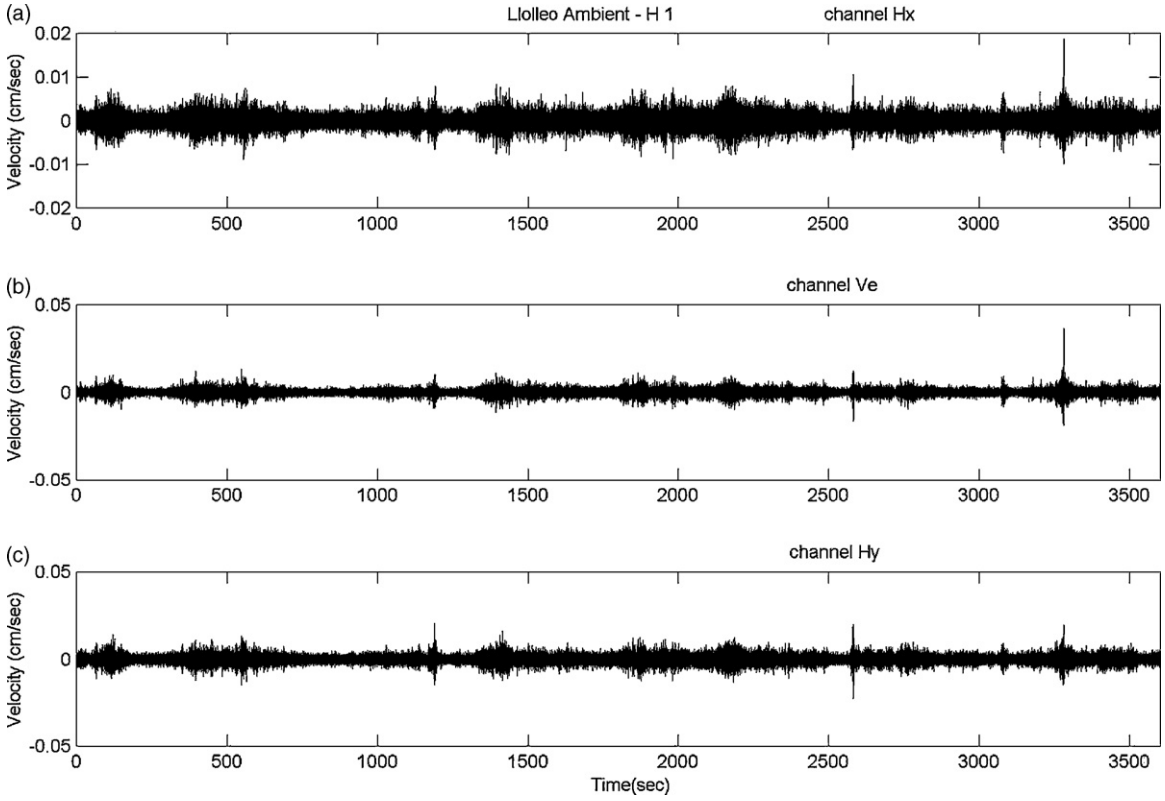

Fig. 18. Time records of microtemors.

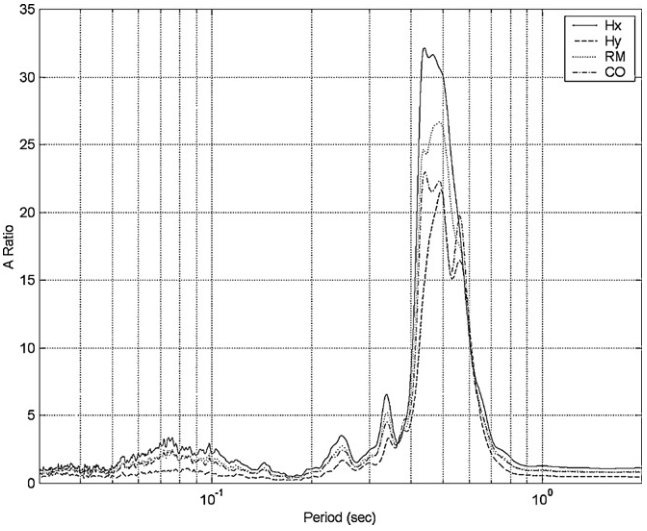

Fig. 19. H/V spectral ratios from microtremors.

An additional power spectral density (CO) was evaluated for the complex combination of the horizontal time records as:

$$\mathrm{CO} = \frac{\mathrm{NS}(t) + i\mathrm{EW}(t)}{2} \tag{11}$$

Prior to performing the H/V ratio a small scalar value was added to the Power Spectral Density of the vertical records to eliminate amplification caused by near division by zero. A value of 1% of the maximum value of the Power Spectral Density of the vertical records was found to give good results without affecting the amplitude ratios.

The H/V ratios using the original and combined horizontal power spectrum are presented in Fig. 19, where it is observed that the four analyzed H/V ratios provide similar results suggesting that the recorded ambient vibrations are homogeneously distributed in all directions. It can be seen that there is a clear peak between 0.42 and 0.48 s, with the second peak at 0.32 s and the third at 0.25 s. The maximum amplification occurs around 0.45 s. It is important to mention that the site is far from any industrial source of noise and that measurements carried out at different time of the day and also at different time of the year provided the same fundamental period around 0.45 s.

This amplification function is quite different from the one obtained previously via the ratio between the response spectra of ground surface and bedrock. However, it identifies the same fundamental period of $T = 0.45$ s, shown by the average empirical transfer function of the site.

12. H/V spectral ratio applied to seismic records

Seismic acceleration records with a peak horizontal acceleration at the ground surface greater than 0.001 g were selected for this study. This permitted the use of 16 recorded earthquakes with good signal to noise ratios.

For each component of the recorded acceleration at the ground surface, the velocity response spectra were computed followed by the H/V spectral ratio. The results obtained for each earthquake are shown in Figs. 20 and 21 for the East–West and North–South horizontal components, respectively, while the average of all the data is shown in Fig. 22. It is interesting to notice that the results for the different earthquake records have some significant differences and that there are also clear dif-

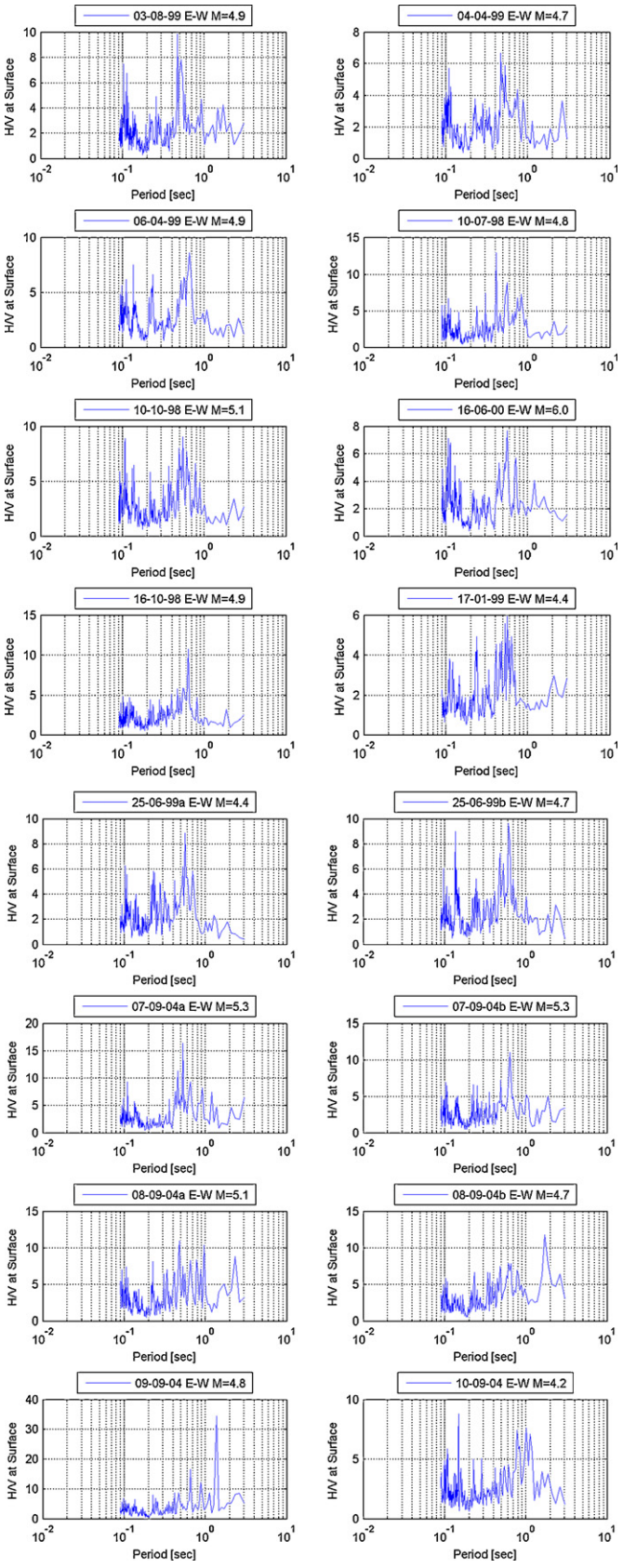

Fig. 20. H/V spectral ratio at the ground surface (E–W).

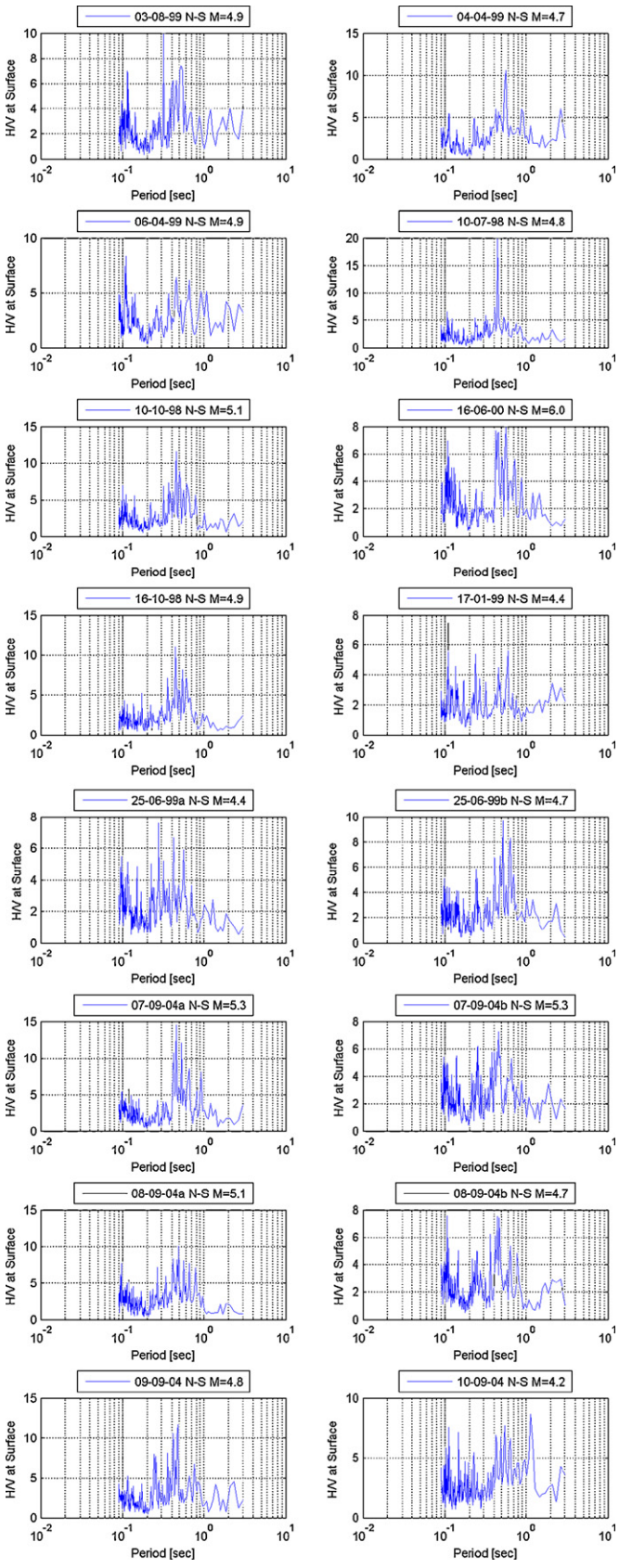

Fig. 21. H/V spectral ratio at the ground surface (N–S).

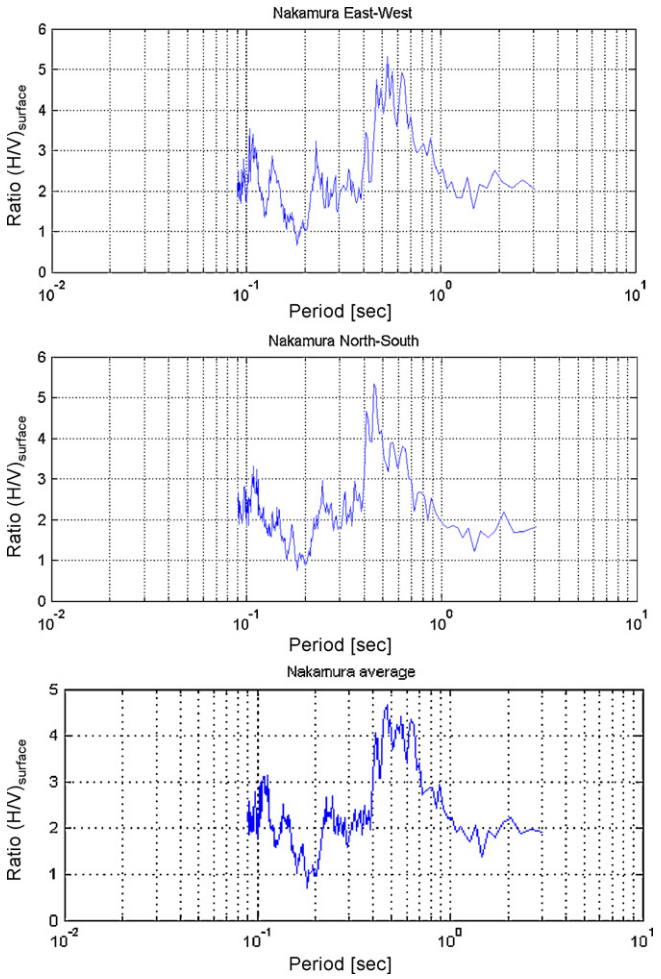

Fig. 22. Average H/V spectral ratio at the ground surface.

ferences for the same earthquake between the results for the East–West and North–South components. If the peaks corresponding to the earthquakes of large magnitude occurred at longer periods than those of the smaller earthquakes this could perhaps be explained by nonlinear soil behavior. Unfortunately, there is no clear trend in this direction. Moreover, even for the strongest motion of magnitude 6, the peak acceleration at the bedrock is of the order of 0.008 g and at the surface 0.1 g, with very small strains and essentially linear soil behavior. It should also be noticed that the highest amplitude peak does not occur at the first peak, corresponding to the longer period or first predominant frequency. It is observed that in most of the cases, the maximum peak occurs consistently in the range of 0.4–0.5 s, and from the average plotted in Fig. 22, it is possible to identify a peak around a period of $T = 0.48$ s, which is coincident with the result obtained using microtremors. Nevertheless, other important peaks can also be identified, suggesting a broad band frequency response.

For the Llolleo site, the acceleration histories at bedrock are available. The ratio, S_{HB}/S_{VB}, that Nakamura's method assumes equal to unity, has been computed and the results are presented in Fig. 23 for the average of all earthquakes. Since this ratio fluctuates between 0.8 and 2.6, the H/V spectral ratio defined by Nakamura is definitely affected, changing at different frequencies the amplitude of the amplification.

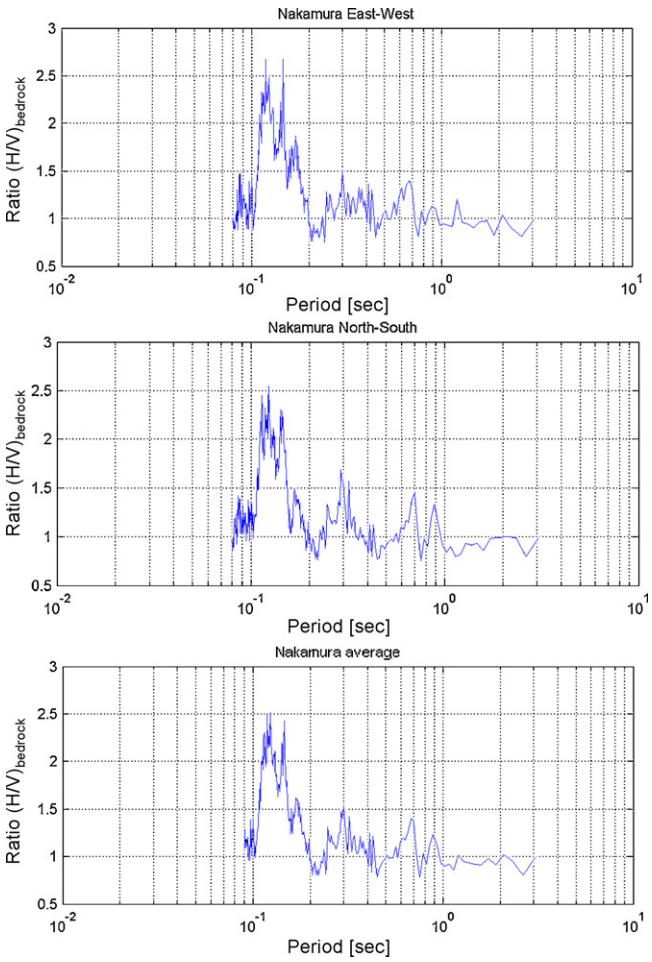

Fig. 23. Average H/V spectral ratio at the bedrock.

13. Conclusions

The main results of the studies conducted using recorded small and medium earthquakes (accelerations and pore water pressures) and measurements of microtremors (ambient vibrations) at Llolleo down-hole array indicate that:

- The dynamic pore water pressures recorded in fine-grained soils are correlated with the vertical acceleration history and therefore, associated with compressional waves traveling throughout the saturated soil deposit.
- The average empirical transfer function of the site, surface-bedrock, obtained from the recorded earthquakes does not show the theoretical natural period computed with the complete profile of shear wave velocities. However, it is possible to identify a natural period that coincides with the theoretical period computed only with the soil properties of the upper 20 m. These results obtained from small to medium seismic events suggest that, in the seismic response at the ground surface, the upper weaker soil layers seem to be the most relevant.
- The average empirical transfer function of the site shows several peaks of amplifications, suggesting that the actual site effect is influenced by a broad band of frequencies. The singularities of each input motion amplify any of these natural frequencies. From an engineering point of view, this finding is very important because structures can undergo resonance at the higher frequencies of the soil deposit, which are normally not considered in dynamic analysis.
- The H/V spectral ratio obtained from microtremors and those corresponding to actual, relatively small, earthquakes for which the soil behavior is essentially linear, show a predominant amplification peak around a period of 0.45 s and seem to be consistent in this respect. This maximum amplification occurs also at the same or very similar period in the ratio of the response spectra of the motions recorded at the free surface and at bedrock.
- The H/V spectral ratios for the small earthquakes show a number of additional peaks with smaller amplitude at higher periods that do not agree with the results of ambient vibrations.
- The H/V spectral ratios and the ratios of the response spectra have some similarities but also some clear differences.
- The H/V spectral ratios and the ratios of response spectra vary substantially from one earthquake record to another, without any clear trend related to the earthquake magnitude, and from one component to the other (North–South and East–West) for the same earthquake.

Acknowledgements

The research project associated with the installation of the Llolleo borehole array has been only possible by the financial support provided by the Fondo Nacional de Investigación Científica y Tecnológica, FONDECYT, under the grant no. 1970440. Additionally, the author wants to thank the support provided by the Milenio Project Seismotectonic and Seismic Risk that made possible this article. The author also wants to thank the very useful comments done by Prof. Jose Roësset.

References

Aki, K., 1993. Local site effects on weak and strong ground motion. Tectonophysics 218, 93–111.
Astroza, M., Monge, J., Varela, J., 1993. Intensities in the Metropolitan Region and Central Coast caused by the earthquake of March 3 (in Spanish). In: R. Flores (Ed.), Seismic Engineering, the Chilean earthquake of March 3, 1985.
Bard, P.-Y., 1999. Microtremor measurements: a tool for site effect estimation. In: Proceedings of the 2nd International Symposium on the Effects of Surface Geology on Seismic Motion. Yokohama, Japan.
Bonilla, L., Steidl, J., Lindley, G., Tumarkin, A., Archuleta, R., 1997. Site amplification in the San Fernando Valley, California: variability of site-effect estimation using the S-Wave, Coda, and H/V methods. Bull. Seism. Soc. Am. 87 (3), 710–730.
Borcherdt, R., 1970. Effect of local geology on ground motion near San Francisco Bay. Bull. Seism. Soc. Am. 60 (1), 29–61.
Borcherdt, R., 1994. Estimates of site-dependent response spectra for design (methodology and justification). Earthquake Spectra 10 (4), 617–653.
Borcherdt, R., 2002. Empirical evidence for acceleration-dependent amplification factors. Bull. Seism. Soc. Am. 92 (2), 761–782.
Celebi, M., Prince, J., Dietel, C., Onate, M., Chavez, G., 1987. The culprit in Mexico city—amplification of motions. Earthquake Spectra 3 (2), 315–328.
Dobry, R., Iai, S., 2000. Recent developments in the understanding of earthquake site response and associated seismic code implementation. Key note paper. Proceedings of the International Conference on Geotechnical and Geological Engineering, vol. 1. Australia, pp. 186–219.
Dobry, R., Ramos, R., Power, M., 1999. Site factors and site categories in seismic codes. Technical Report MCEER-99-0010. University at Buffalo.
Field, E., Hough, S., 1997. The variability of PSV response spectra across a dense array deployed during the Northridge aftershock sequence. Earthquake Spectra 13 (2), 243–256.
Field, E., Jacob, K., 1993. The theoretical response of sedimentary layers to ambient seismic noise. Geophys. Res. Lett. (20), 2925–2928.
Field, E., Jacob, K., 1995. A comparison and test of various site-response estimation techniques, including three that are not reference-site dependent. Bull. Seism. Soc. Am. 85 (4), 1127–1143.
Field, E., Hough, S., Jacob, K., 1990. Using microtremors to assess potential earthquake site response: a case study in Flushing Meadows, New York City. Bull. Seism. Soc. Am. 80 (6), 1456–1480.
Hudson, D., 1956. Response spectrum technique in engineering seismology. Proceedings of the 2nd World Conference on Earthquake Engineering.
Hudson, D., 1979. Reading and Interpreting Strong Motion Accelerograms. Earthquake Engineering Research Institute, California Institute of Technology.
Ishihara, K., 1982. Evaluation of soil properties for use in earthquake response analysis. International Symposium on Numerical Models in Geomechanics. Zurich.
Ishihara, K., 1993. Liquefaction and flow failure during earthquakes. 33rd Rankine Lecture. Geotechnique 43 (3), 351–415.

Konno, K., Ohmachi, T., 1998. Ground-motion characteristics estimated from spectral ratio between horizontal and vertical components of microtremor. Bull. Seism. Soc. Am. 88 (1), 228–241.
Lachet, C., Bard, P., 1994. Numerical and theoretical investigations on the possibilities and limitations of Nakamura's technique. J. Phys. Earth (42), 377–397.
Lermo, J., Chávez-García, J., 1993. Site effect evaluation using spectral ratios with only one station. Bull. Seism. Soc. Am. 83 (5), 1574–1594.
Midorikawa, S., Matsuoka, M., Sakugawa, K., 1994. Site effect on strong-motion records observed during the 1987 Chiba-Ken-Toho-Oki, Japan earthquake. In: Proceedings of the 9th Japan Earthquake Engineering Symposium, vol. 3, pp. E085–E090.
Mohraz, B., 1976. A study of earthquake response spectra for different geological conditions. Bull. Seism. Soc. Am. 66 (3), 915–935.
Nakamura, Y., 1989. A method for dynamic characteristics estimation of subsurface using microtremor on the ground surface. Q. Rep. RTRI 30 (1), 25–33.
Roësset, J., 1977. Soil amplification of earthquakes. In: C.S. Desai and J.T. Christian (Eds.). Numerical Methods in Geotechnical Engineering. McGraw-Hill, New York (Chapter 19, pp. 639–682).
Roësset, J., Whitman, R., 1969. Theoretical background for amplification studies. MIT Research Report No. R69-15.
Rovelli, A., Singh, S., Malagnini, L., Amato, A., Cocco, M., 1991. Feasibility of the use of microtremors in estimating site response during earthquakes: some test cases in Italy. Earthquake Spectra 7 (4), 551–560.
Safak, E., 1991. Problems with Using Spectral Ratios to Estimate Site Amplification. Proceedings of 4th International Conference on Seismic Zonation, vol. II. Stanford, California, pp. 277–284.
Saita, J., Matsuoka, M., Yamazaki, F., Shabestari, K., 2001. Site response characteristic of seismic stations in Japan based on microtremor observation and strong motion records. Proceedings of 8th East Asia-Pacific Conference on Structural Engineering and Construction. Singapore.
Sarrazin, M., Vanmarcke, E., Roesset, J., 1969. The use of amplification functions to derive response spectra including the effect of local soil conditions. Report R69-48. Department of Civil Engineering, MIT, USA.
Seed, H., 1987. Design problems in soil liquefaction. J. Geotech. Eng., ASCE 113 (8), 827–845.
Seed, H., Idriss, I., 1969. Influence of soil conditions on ground motions during earthquakes. J. Soil Mech. Foundations Division, ASCE 95 (SM1).
Seed, H., Idriss, I., 1970. Soil moduli and damping factors for dynamic response analyses. Report EERC 70-10. University of California, Berkeley.
Seed, B., Murarka, R., Lymer, J., Idriss, I., 1976. Relationships of maximum acceleration, maximum velocity, distance from source, and local site conditions for moderately strong earthquakes. Bull. Seism. Soc. Am. 66 (4), 1323–1342.
Seed, H., Romo, M., Sun, J., Jaime, A., Lysmer, J., 1988. Relationships between soil conditions and earthquake ground motions. Earthquake Spectra 4, 687–729.
Singh, S., Ordaz, M., 1993. On the origin of long coda observed in the lake-bed strong-motion records of Mexico City. Bull. Seism. Soc. Am. 83, 1298–1306.